Macula structural and vascular differences in glaucoma eyes with and without high axial myopia

Jasmin Rezapour, MD[1,2], Christopher Bowd, PhD[1], Jade Dohleman[1], Akram Belghith, PhD[1], James A. Proudfoot,MSc[1], Mark Christopher, PhD[1], Leslie Hyman, PhD[3], Jost B. Jonas, MD[4], Rafaella C. Penteado, MD[1], Sasan Moghimi, MD[1], Huiyuan Hou, MD[1], Massimo A. Fazio, PhD[5,6], Robert N. Weinreb, MD[1], Linda M. Zangwill, PhD[1]

1 Hamilton Glaucoma Center, Shiley Eye Institute, Viterbi Family Department of Ophthalmology, UC San Diego, La Jolla, CA, United States
2 Department of Ophthalmology, University Medical Center of the Johannes Gutenberg University Mainz, Germany
3 Wills Eye Hospital, Thomas Jefferson University, Philadelphia, PA, United States
4 Department of Ophthalmology, Medical Faculty Mannheim, Heidelberg University, Mannheim, Germany
5 Department of Ophthalmology and Vision Science, School of Medicine, The University of Alabama at Birmingham, Birmingham, AL, United States
6 Department of Biomedical Engineering, School of Engineering, The University of Alabama at Birmingham, Birmingham, AL, United States

Word count: 2907

*Corresponding author:
Linda M. Zangwill
9500 Gilman Drive
La Jolla, CA 92093-0946
Shiley Eye Institute/Hamilton Glaucoma Center
Viterbi Family Department of Ophthalmology
University of California, San Diego
T: (858) 534-7686
Email: lzangwill@health.ucsd.edu

Precis

In glaucoma eyes, macula ganglion cell thickness measures were significantly associated with severity of glaucoma but not axial length suggesting that macula OCT parameters may be useful in detecting glaucoma in eyes with high myopia.

Abstract

Aims

To assess the thickness of various retinal layers, and the superficial vessel density (sVD) in the macula of glaucomatous eyes and their associations with axial length (AL) and visual field mean deviation (VFMD) to identify parameters useful for glaucoma management in myopic eyes.

Methods

248 glaucoma patients (401 eyes) participating in the Diagnostic Innovations in Glaucoma Study observational cohort representing 3 axial myopia groups (non-myopia: n=146 eyes; mild myopia: n=208 eyes; high myopia (AL>26 mm): n=47 eyes) who completed macular OCT and OCT-Angiography imaging were included. The cross-sectional associations of AL and VFMD with the thickness of the ganglion cell inner plexiform layer (GCIPL), macular retinal nerve fiber layer (mRNFL), ganglion cell complex (GCC), sVD and macular choroidal thickness (mCT) were evaluated.

Results

Thinner Global GCIPL and GCC were significantly associated with worse VFMD (R^2=35.1%; and R^2=33.4%; respectively p<0.001), but not with AL (all p>0.350). Thicker mRNFL showed a weak association with increasing AL (R^2=3.4%; p=0.001) and a positive association with VFMD (global R^2=20.5%; p<0.001). Lower sVD was weakly associated with increasing AL (R^2=2.3%; p=0.016) and more strongly associated with more severe glaucoma VFMD (R^2=31.8%; p<0.001). Thinner mCT was associated with increasing AL (R^2=17.3% p<0.001) and not associated with VFMD (P=0.262). mRNFL was thickest while mCT was thinnest in all sectors of high myopic eyes.

Conclusions

GCIPL and GCC thinned with increasing severity of glaucoma but were not significantly associated with axial length. GCIPL and GCC thickness may be useful clinical parameters to identify glaucoma in myopic eyes.

Introduction

With its potential vision threatening risk and with its prevalence increasing globally, myopia, especially high myopia, has become a major concern around the world.[1]

Although optical coherence tomography (OCT) based measurements of peripapillary retinal nerve fiber layer (pRNFL) thickness can accurately discriminate between healthy and glaucomatous eyes,[2] there is concern that in myopic eyes (and especially in high myopic eyes) the diagnostic accuracy of OCT measures is decreased. Optic disc changes in myopic eyes such as morphologic changes in the parapapillary region and optic disc enlargement pose significant challenges to the use of optical imaging and clinical optic disc evaluation to detect and monitor glaucoma (Figure 1).[1,3] This is due in part to difference in the regional arrangement of the peripapillary retinal nerve fibers between myopic eyes and emmetropic eyes that may result in sectoral values incorrectly classified as outside normal limits by instrument-specific software analysis in healthy myopic eyes.[4 5]

Approximately 50% of the retinal ganglion cells are concentrated within 10 degree of the fovea[6] making the macula an useful region for diagnosing optic neuropathies including glaucoma, especially in myopic eyes because myopic axial elongation primarily affects the optic nerve head region. Previous studies have reported that early glaucomatous damage can be detected in the macula region[7] and that measurements of the ganglion cell inner plexiform layer (GCIPL) can be used for detecting glaucoma in highly myopic eyes.[8-12] However, little information is available about differences in the topographic distribution of the thickness of the various macular retinal layers and the retinal vessel density in glaucomatous eyes with and without myopia. Sectoral measurements of the underlying macular vasculature may offer additional insight into differences in glaucomatous eyes with and without myopia.

Several studies using OCT-Angiography (OCTA) have demonstrated a strong relationship between macular capillary density and the severity of glaucoma.[13 14] Furthermore recent studies have reported the peripapillary choroid to be thinner in highly myopic eyes compared

to non-myopic eyes.[15 16] However, few studies have assessed macular choroidal thickness in highly myopic eyes[17 18] and to date, to the best of our knowledge, no study has documented the local distribution of macular choroidal thickness in glaucomatous eyes with and without high myopia.

The purpose of this study was to characterize the local distribution of GCIPL, GCC, macular retinal nerve fiber layer (mRNFL), choroidal thickness and vessel density in glaucoma eyes with and without axial myopia. By better understanding how the topographic distribution of these parameters varies with axial length and severity of disease, macula parameters that may be useful for detecting and monitoring glaucoma in myopic eyes can be identified.

Methods

Study Sample

This cross-sectional study included all glaucoma patients enrolled in the University of California, San Diego Diagnostic Innovations in Glaucoma Study (DIGS; clinicaltrials.gov identifier NCT00221897) with available axial length measurements and good quality macula OCT scans acquired between 2015 and 2020. The study was approved by the institutional review board of the University of California San Diego and according to the tenets of the Declaration of Helsinki written informed consent was obtained from all patients. As described previously;[19] participants underwent a complete ophthalmologic examination including assessment of refractive error, axial length measurement (IOLMaster, Carl Zeiss Meditec, Dublin, CA), visual field testing, simultaneous stereophotography of the optic disc and macula, and macular OCT and OCTA imaging. Study participants were ≥18 years with best-corrected visual acuity ≥20/40 and open anterior chamber angles at baseline.

Visual field (VF) testing was performed using the standard Humphrey Field Analyzer 24-2 Swedish interactive thresholding algorithm. Repeatable glaucomatous VF damage was defined as the presence of glaucomatous optic nerve head (ONH) damage based on masked assessment by two trained observers and glaucomatous VF damage.[19] ONH

stereophotographs of highly myopic eyes were graded for glaucoma by two experts (CB and JR) after training with a senior consultant (JBJ). Diagnosis was defined by consensus between the two graders and adjudication by the senior consultant in case of disagreement.

Myopia definition

Because a change in refractive error can occur after refractive or cataract surgery, myopia was classified by axial length into the following 3 groups.

-No myopia: axial length ≤ 24.0 mm

-Mild myopia: 24.0mm < axial length ≤ 26.0 mm

-High myopia: axial length > 26.0 mm

Optical coherence tomography and optical coherence tomography angiography imaging

OCT imaging of the macula was performed with the Spectralis OCT (version 6.10; Heidelberg Engineering Inc, Heidelberg, Germany). Details of this instrument have been previously described.[14] Macula horizontal posterior pole (p-Pole) scans covering an area of 30° x 25° (6 x 6 mm) were obtained. GCIPL, mRNFL and GCC (GCIPL + mRNFL) thickness measurements were generated from each retinal layer from the central 1-, 3-, and 6-mm circles as inner rings (1- and 3-mm circle) and outer rings (3- and 6-mm circle) according to the Early Treatment Diabetic Retinopathy Study defined sectors (temporal, superior, nasal, and inferior).

OCTA imaging of the macula was performed with the Avanti AngioVue OCT system (version 2017.1.0.151; Optovue, Inc., Fremont CA, USA).[20] Macular whole image vessel density was calculated on a 3 x 3 mm^2 field macula scan (304 B-scans x 304 A-scans per B-scan) centered on the fovea. Whole image vessel density of the temporal, superior, nasal, and inferior sectors were reported. Macular parafoveal superficial VD (sVD) was calculated within

an annulus centered on the fovea, with an inner diameter of 1 mm and an outer diameter of 2.5 mm.

All images were reviewed by the Imaging Data Evaluation and Analysis (IDEA) Reading Center for image quality, and accurate segmentation of the mRNFL, ganglion cell layer (GCL), and inner plexiform layer (IPL). The automated Spectralis software segmentation was manually corrected if needed, according to the standard IDEA Reading Center protocols.[19]

Choroidal thickness measurement using deep learning

As choroidal thickness is not available from standard software, custom deep learning-based software was developed to automatically measure mCT.[21] A trained grader (JR) manually segmented the Bruch's Membrane (BM) / RPE complex and the posterior boundary of the choroid in 120 p-Pole scans in the SPX software (version 1.9.204.0; Heidelberg Engineering Inc, Heidelberg, Germany) in a subset of 20 eyes, which was used as ground truth to train a deep convolutional neural network model (BCDU-Net).[22] Two thousand two hundred fifty seven scans (753 eyes) with automated choroid segmentation were reviewed for accuracy (JR). The overall performance of the deep learning algorithm for segmenting the choroid was very good with 400/401 (99.8%) eyes included (no myopia: 146/146 (100%), mild myopia: 208/208 (100%) and high myopia: 46/47 (97.9%)).

Macular choroidal thickness (mCT) was obtained for the inner and outer rings of the macular p-Pole scans defined above. Each ring was subdivided into temporal, superior, nasal, and inferior sectors and global and sectoral choroidal thickness was calculated. The MCT was defined as the perpendicular distance between the posterior border of BM / retinal pigment epithelium (RPE) complex and the posterior boundary of the choroid.

Statistical Analyses

Data is presented as mean (95% confidence interval (CI)) and count (percentage) for continuous and categorical variables, respectively. Patient and eye characteristics were compared across myopia groups using analysis of variance (ANOVA) and chi-squared tests for continuous and categorical patient-level variables (respectively) and linear mixed effects models for continuous eye-level variables, with a random intercept to account for within-patient correlation. Univariable and age and VFMD adjusted multivariable models were applied to evaluate the association between axial length and ocular parameters. P-values less than 0.05 were considered statistically significant. All statistical analyses were performed using R (version 3.6.3).

Results

Four-hundred-one glaucoma eyes of 248 patients were included with 146 eyes (87 patients) in the non-myopic group, 208 eyes (125 patients) in the mild myopic group, and 47 highly myopic eyes (36 patients) (Table 1). All p-values are reported as age-adjusted.

	No axial myopia (n=87; 146 eyes)	Mild axial myopia (n=125; 208 eyes)	High axial myopia (n=36; 47 eyes)	Overall (n=248, 401 eyes)	P-value	Age-adjusted p-value
Age	76.5 (74.1, 78.8	73.0 (71.1, 75.0)	67.5 (63.7, 71.4)	73.4 (72.0, 74.8)	<0.001[1,2,3]	
Gender						
Female	55 (63.2%)	55 (44.0%)	13 (36.1%)	123 (49.6%)	0.005[1,2]	
Male	32 (36.8%)	70 (56.0%)	23 (63.9%)	125 (50.4%)		
Race						
African Descent	21 (24.1%)	22 (17.6%)	3 (8.3%)	46 (18.5%)	0.057[2,3]	
Asian Descent	7 (8.0%)	15 (12.0%)	10 (27.8%)	32 (12.9%)		
European Descent	57 (65.5%)	84 (67.2%)	21 (58.3%)	162 (65.3%)		
Axial length (mm)	23.4 (23.3, 23.6)	24.9 (24.8, 25.0)	26.5 (26.3, 26.7)	24.5 (24.4, 24.7)	<0.001[1,2,3]	<0.001[1,2,3]
SE (dpt)	−0.00 (−0.41, 0.41)	−1.50 (−1.85, −1.16)	−2.84 (−3.42, −2.26)	−1.12 (−1.44, −0.79)	<0.001[1,2,3]	<0.001[1,2,3]
CCT	537.9 (529.5, 546.3)	534.5 (527.4, 541.7)	535.5 (523.0, 548.1)	535.9 (530.2, 541.6)	0.803	0.637
VFMD (db)	-5.75 (-7.05, -4.45)	-7.10 (-8.19, -6.00)	-7.18 (-9.32, -5.04)	-6.61 (-7.43, -5.80)	0.251	
IOP (mmHg)	14.6 (13.7, 15.5)	13.8 (13.1, 14.6)	14.1 (12.6, 15.5)	14.1 (13.6, 14.7)	0.423	0.093[1]
Cataract Surgery						
Yes	63 (43.2%)	78 (37.5%)	14 (29.8%)	155 (38.7%)	0.236	
No	83 (56.8%)	130 (62.5%)	33 (70.2%)	246 (61.3%)		
Refractive Surgery						
Yes	0 (0.0%)	12 (5.8%)	2 (4.3%)	14 (3.5%)	0.003[1]	
No	146 (100.0%)	196 (94.2%)	45 (95.7%)	387 (96.5%)		

Table 1: Glaucoma patient and eye characteristics by myopia group.
Results are presented as mean (95% confidence interval) or percentage. Race was compared using a chi-squared test. Continuous variables were compared using ANOVA (for age) or linear mixed models (for eye level data).
No myopia: AL ≤24.0mm; Mild myopia: AL: >24mm and ≤26.0mm; High myopia: AL >26.0mm
Missing 13^a, 2^b, and 8^c values.
[1] No vs. Mild Myopia $p < 0.05$; [2] No vs. High Myopia $p < 0.05$; [3] Mild vs. High Myopia $p < 0.05$
Abbreviations: BMO; Bruch's membrane opening, IOP; intraocular pressure, MD; mean deviation

The participants in the high myopia group were significantly younger (mean [95% CI]) 67.5 [63.7, 71.4] years) than the members of the mild (73.0 [71.1, 75.0] years) myopic group and the non-myopic individuals (76.5 [74.1, 78.8] years) groups ($p<0.001$). There was a trend of a higher proportion of individuals of Asian descent in the high myopia group compared to the no-myopic and the mild myopic group ($p=0.06$).

There was no significant difference in intraocular pressure ($p=0.09$), central corneal thickness ($p=0.64$) and BMO area ($p=0.51$) among the three groups (Table 1). Non-myopes tended ($p=0.131$) to have less severe glaucoma than the mild myopic group and the high myopic group (mean visual field mean deviation (MD) -5.75 dB, -7.10 dB and -7.18 dB, respectively).

Macular Thickness Measurements

A total of 43 eyes were excluded from the analysis for not meeting image quality criteria (Spectralis quality score >15 dB or segmentation failure) with 14/140 (10.1%), 12/220 (5.5%) and 17/64 (26.6%) eyes excluded from the no-, mild- and high-axial myopia groups, respectively. Macular thickness measures are presented in Figure 2 and Supplemental Table 1.

Associations with Axial Length

There were no statistically significant associations between global and sectoral GCC or GCPIL thickness measurements and axial length except for a weak association of the GCIPL outer nasal sector ($R^2=1.9\%$, $p=0.016$). All mRNFL measurements, except for the inner temporal and outer inferior sector were significantly (all $p<0.024$) but relatively weakly (all $R^2 < 5\%$) associated with axial length. We found weak associations between global and sectoral vessel density measurements and axial length (all $R^2 \leq 3.2\%$, all $p<0.05$) and stronger associations between choroidal thickness measures and axial length (R^2 range: 9.6%-19.3%, all $p<0.001$) (Table 2).

	Patients (eyes)	Univariable Regression		Multivariable Regression	
		Estimate	R^2 (p-value)	Estimate	$R^{2(\%)}$ (p-value)
Age	N=248 (401)	-0.26 (-0.59, 0.07)	0.1 (0.121)	-0.25 (-0.58, 0.07)	0.1 (0.130)
VFMD	N=248 (401)	-0.35 (-0.97, 0.27)	0.4 (0.272)	-0.53 (-1.17, 0.12)	0.8 (0.110)
Spectralis GCIPL (µm)					
Global	N=248 (401)	-0.29 (-1.21, 0.63)	0.1 (0.531)	-0.41 (-1.19, 0.36)	0.4 (0.299)
Inner ring	N=248 (401)	-0.32 (-1.58, 0.94)	0.1 (0.618)	-0.36 (-1.42, 0.69)	0.2 (0.498)
Outer ring	N=248 (401)	-0.26 (-0.92, 0.40)	0.2 (0.443)	-0.45 (-1.05, 0.14)	0.7 (0.136)
Inner temporal	N=248 (401)	0.14 (-1.26, 1.54)	0.0 (0.843)	0.29 (-0.86, 1.43)	0.1 (0.625)
Inner superior	N=248 (401)	-0.60 (-1.90, 0.71)	0.3 (0.370)	-0.82 (-2.01, 0.37)	0.6 (0.180)
Inner nasal	N=248 (401)	-0.61 (-1.96, 0.74)	0.3 (0.380)	-0.76 (-1.99, 0.47)	0.5 (0.226)
Inner inferior	N=248 (401)	-0.21 (-1.69, 1.26)	0.0 (0.780)	-0.11 (-1.37, 1.15)	0.0 (0.859)
Outer temporal	N=248 (401)	-0.20 (-1.01, 0.62)	0.1 (0.637)	-0.20 (-0.91, 0.51)	0.1 (0.577)
Outer superior	N=248 (401)	-0.21 (-0.92, 0.50)	0.1 (0.567)	-0.47 (-1.14, 0.20)	0.6 (0.170)
Outer nasal	N=248 (401)	-0.49 (-1.28, 0.30)	0.5 (0.225)	-0.92 (-1.66, -0.18)	1.9 (0.016)
Outer inferior	N=248 (401)	-0.18 (-0.84, 0.48)	0.1 (0.595)	-0.27 (-0.90, 0.37)	0.2 (0.411)
Spectralis RNFL (µm)					
Global	N=248 (401)	0.33 (-0.05, 0.71)	0.9 (0.092)	0.59 (0.24, 0.95)	3.4 (0.001)
Inner ring	N=248 (401)	0.32 (0.06, 0.59)	1.8 (0.018)	0.49 (0.22, 0.76)	3.9 (<0.001)
Outer ring	N=248 (401)	0.33 (-0.21, 0.87)	0.5 (0.233)	0.70 (0.21, 1.19)	2.6 (0.005)
Inner temporal	N=248 (401)	0.04 (-0.16, 0.24)	0.1 (0.671)	0.19 (-0.01, 0.39)	1.0 (0.066)
Inner superior	N=248 (401)	0.55 (0.18, 0.92)	2.7 (0.004)	0.74 (0.35, 1.12)	4.4 (<0.001)
Inner nasal	N=248 (401)	0.44 (0.09, 0.79)	1.9 (0.014)	0.62 (0.25, 0.98)	3.4 (<0.001)
Inner inferior	N=248 (401)	0.27 (-0.09, 0.63)	0.7 (0.141)	0.44 (0.09, 0.80)	1.8 (0.015)
Outer temporal	N=248 (401)	0.07 (-0.13, 0.28)	0.2 (0.483)	0.23 (0.03, 0.44)	1.6 (0.024)
Outer superior	N=248 (401)	0.44 (-0.28, 1.16)	0.5 (0.231)	0.83 (0.15, 1.51)	1.8 (0.017)
Outer nasal	N=248 (401)	0.60 (-0.23, 1.43)	0.6 (0.160)	1.14 (0.36, 1.93)	2.7 (0.004)
Outer inferior	N=248 (401)	0.17 (-0.57, 0.91)	0.1 (0.654)	0.59 (-0.09, 1.26)	0.9 (0.088)
Spectralis GCC (µm)					
Global	N=248 (401)	0.03 (-1.19, 1.25)	0.0 (0.964)	0.18 (-0.88, 1.25)	0.0 (0.737)
Inner ring	N=248 (401)	0.00 (-1.41, 1.41)	0.0 (0.998)	0.12 (-1.10, 1.35)	0.0 (0.844)
Outer ring	N=248 (401)	0.07 (-1.04, 1.17)	0.0 (0.909)	0.25 (-0.75, 1.24)	0.1 (0.625)
Inner temporal	N=248 (401)	0.18 (-1.24, 1.61)	0.0 (0.800)	0.47 (-0.72, 1.66)	0.2 (0.438)
Inner superior	N=248 (401)	-0.06 (-1.59, 1.48)	0.0 (0.943)	-0.08 (-1.53, 1.36)	0.0 (0.910)
Inner nasal	N=248 (401)	-0.16 (-1.68, 1.37)	0.0 (0.840)	-0.14 (-1.58, 1.31)	0.0 (0.852)
Inner inferior	N=248 (401)	0.06 (-1.68, 1.80)	0.0 (0.947)	0.33 (-1.20, 1.85)	0.1 (0.676)
Outer temporal	N=248 (401)	-0.12 (-1.05, 0.82)	0.0 (0.805)	0.03 (-0.80, 0.87)	0.0 (0.940)
Outer superior	N=248 (401)	0.23 (-1.07, 1.53)	0.0 (0.725)	0.36 (-0.87, 1.58)	0.1 (0.569)
Outer nasal	N=248 (401)	0.12 (-1.31, 1.55)	0.0 (0.873)	0.22 (-1.13, 1.56)	0.0 (0.750)
Outer inferior	N=248 (401)	-0.02 (-1.30, 1.27)	0.0 (0.978)	0.31 (-0.88, 1.51)	0.1 (0.608)
Avanti GCC (µm)					
Whole image	N=204 (317)	-0.04 (-1.44, 1.36)	0.0 (0.954)	0.02 (-1.23, 1.26)	0.0 (0.979)
Parafovea	N=204 (317)	-0.15 (-1.64, 1.33)	0.0 (0.839)	-0.13 (-1.45, 1.19)	0.0 (0.850)
Temporal	N=204 (317)	-0.11 (-1.60, 1.38)	0.0 (0.888)	0.07 (-1.20, 1.33)	0.0 (0.920)
Superior	N=203 (316)	-0.15 (-1.81, 1.50)	0.0 (0.857)	-0.16 (-1.76, 1.43)	0.0 (0.839)
Nasal	N=204 (317)	-0.11 (-1.71, 1.48)	0.0 (0.891)	-0.25 (-1.75, 1.26)	0.0 (0.750)
Inferior	N=204 (316)	-0.31 (-2.14, 1.52)	0.0 (0.739)	-0.28 (-1.89, 1.34)	0.0 (0.739)
Avanti Vessel Density (%)					
Whole image	N=204 (317)	-0.35 (-0.87, 0.17)	0.7 (0.191)	-0.54 (-0.97, -0.10)	2.3 (0.016)
Parafovea	N=204 (317)	-0.42 (-0.97, 0.13)	0.9 (0.138)	-0.63 (-1.09, -0.18)	2.8 (0.007)
Temporal	N=204 (317)	-0.38 (-0.95, 0.18)	0.7 (0.183)	-0.49 (-0.96, -0.01)	1.5 (0.046)
Superior	N=203 (316)	-0.31 (-0.88, 0.26)	0.4 (0.293)	-0.59 (-1.09, -0.09)	2.0 (0.022)
Nasal	N=204 (317)	-0.48 (-1.05, 0.08)	1.1 (0.096)	-0.75 (-1.24, -0.25)	3.2 (0.004)
Inferior	N=204 (316)	-0.57 (-1.26, 0.11)	1.0 (0.102)	-0.78 (-1.36, -0.21)	2.7 (0.008)
Spectralis Choroid (µm)					
Global	N=247 (400)	-10.95 (-14.96, -6.94)	8.9 (<0.001)	-15.17 (-18.96, -11.38)	17.3 (<0.001)
Inner Ring	N=247 (400)	-11.51 (-16.18, -6.84)	7.5 (<0.001)	-16.04 (-20.49, -11.58)	14.6 (<0.001)
Outer Ring	N=247 (400)	-10.81 (-14.70, -6.92)	9.2 (<0.001)	-14.97 (-18.64, -11.30)	17.9 (<0.001)
Inner Temporal	N=247 (400)	-8.05 (-12.53, -3.57)	4.1 (<0.001)	-12.33 (-16.64, -8.02)	9.6 (<0.001)
Inner Superior	N=247 (400)	-12.56 (-17.72, -7.40)	7.3 (<0.001)	-17.30 (-22.26, -12.34)	13.8 (<0.001)
Inner Nasal	N=247 (400)	-16.87 (-22.38, -11.36)	11.1 (<0.001)	-21.73 (-27.06, -16.41)	17.9 (<0.001)
Inner Inferior	N=247 (400)	-9.28 (-14.19, -4.37)	4.5 (<0.001)	-14.19 (-18.87, -9.51)	10.8 (<0.001)
Outer Temporal	N=247 (400)	-6.56 (-10.30, -2.83)	4.0 (<0.001)	-11.03 (-14.47, -7.60)	11.8 (<0.001)
Outer Superior	N=247 (400)	-13.07 (-17.89, -8.24)	8.9 (<0.001)	-17.45 (-22.12, -12.78)	15.5 (<0.001)
Outer Nasal	N=247 (400)	-14.37 (-18.70, -10.04)	12.8 (<0.001)	-18.10 (-22.34, -13.86)	19.3 (<0.001)
Outer Inferior	N=247 (400)	-10.15 (-14.80, -5.50)	6.0 (<0.001)	-14.92 (-19.32, -10.51)	13.1 (<0.001)

Table 2. Ocular associations with axial length

*Linear mixed models slope estimates (with 95% confidence intervals) from univariable and multivariable models adjusted for age and VFMD. ^R^2 reported as a percentage

Abbreviations: GCC; Ganglion cell complex, GCIPL; Ganglion cell inner plexiform layer, RNFL; Retinal nerve fiber layer, VFMD; Visual field mean deviation

Associations with Severity of Glaucoma (Visual Field MD)

In multivariable models adjusted for age and axial length we found relatively strong associations between thinner global and sectoral GCIPL measures and worse VFMD (R^2 range: 14.0%-38.1%, all $p<0.001$). Thinner mRNFL was also significantly associated with worse VFMD in all sectors (R^2 range: 3.1%-23.8%, all $p<0.001$) with exception of the inner nasal and temporal sectors ($p>0.285$). Thinner global and sectoral Spectralis and Avanti GCC measures were significantly associated with worse VFMD (R^2 range: from 20.2% to 37.0% and 18.6% to 35.4%, all $p<0.001$, respectively). In addition, we found a relatively strong association between lower macular vessel density and worse VFMD (R^2 ranged from 20.3% to 33.2%, all $p<0.001$). Macular choroidal thickness was not associated with VFMD (Table 3).

	Patients (eyes)	Univariable Regression		Multivariable Regression	
		Estimate	R^2 (p-value)	Estimate	$R^{2(\%)}$ (p-value)
Age	N=248 (401)	-0.006 (-0.025, 0.014)	0.0 (0.558)	-0.005 (-0.024, 0.015)	0.0 (0.636)
Axial length	N=248 (401)	0.002 (-0.007, 0.010)	0.0 (0.679)	0.001 (-0.008, 0.009)	0.0 (0.860)
Spectralis GCIPL (µm)					
Global	N=248 (401)	0.88 (0.77, 0.99)	35.7 (<0.001)	0.86 (0.75, 0.97)	35.1 (<0.001)
Inner ring	N=248 (401)	1.25 (1.10, 1.40)	38.1 (<0.001)	1.23 (1.08, 1.38)	37.5 (<0.001)
Outer ring	N=248 (401)	0.51 (0.42, 0.59)	23.7 (<0.001)	0.49 (0.41, 0.57)	23.1 (<0.001)
Inner temporal	N=248 (401)	1.40 (1.23, 1.58)	38.6 (<0.001)	1.39 (1.21, 1.57)	38.1 (<0.001)
Inner superior	N=248 (401)	1.02 (0.85, 1.19)	24.0 (<0.001)	0.99 (0.82, 1.16)	23.1 (<0.001)
Inner nasal	N=248 (401)	1.07 (0.90, 1.24)	25.1 (<0.001)	1.05 (0.88, 1.21)	24.4 (<0.001)
Inner inferior	N=248 (401)	1.45 (1.25, 1.64)	35.6 (<0.001)	1.43 (1.23, 1.62)	34.8 (<0.001)
Outer temporal	N=248 (401)	0.73 (0.63, 0.84)	31.5 (<0.001)	0.72 (0.61, 0.82)	30.7 (<0.001)
Outer superior	N=248 (401)	0.43 (0.33, 0.53)	14.7 (<0.001)	0.41 (0.31, 0.51)	13.8 (<0.001)
Outer nasal	N=248 (401)	0.46 (0.35, 0.56)	13.6 (<0.001)	0.43 (0.33, 0.53)	13.0 (<0.001)
Outer inferior	N=248 (401)	0.40 (0.31, 0.49)	14.7 (<0.001)	0.39 (0.30, 0.48)	14.0 (<0.001)
Spectralis RNFL (µm)					
Global	N=248 (401)	0.26 (0.21, 0.31)	18.8 (<0.001)	0.27 (0.22, 0.32)	20.5 (<0.001)
Inner ring	N=248 (401)	0.08 (0.04, 0.12)	3.5 (<0.001)	0.09 (0.05, 0.13)	4.4 (<0.001)
Outer ring	N=248 (401)	0.44 (0.37, 0.51)	26.2 (<0.001)	0.45 (0.38, 0.52)	27.5 (<0.001)
Inner temporal	N=248 (401)	0.01 (-0.02, 0.04)	0.1 (0.599)	0.02 (-0.01, 0.05)	0.3 (0.285)
Inner superior	N=248 (401)	0.09 (0.04, 0.15)	2.5 (0.001)	0.10 (0.05, 0.16)	3.1 (<0.001)
Inner nasal	N=248 (401)	0.02 (-0.04, 0.07)	0.1 (0.543)	0.03 (-0.03, 0.08)	0.3 (0.315)
Inner inferior	N=248 (401)	0.19 (0.13, 0.25)	10.4 (<0.001)	0.20 (0.14, 0.25)	11.3 (<0.001)
Outer temporal	N=248 (401)	0.05 (0.02, 0.09)	2.8 (<0.001)	0.06 (0.03, 0.10)	4.0 (<0.001)
Outer superior	N=248 (401)	0.52 (0.42, 0.62)	20.1 (<0.001)	0.53 (0.43, 0.63)	21.0 (<0.001)
Outer nasal	N=248 (401)	0.63 (0.53, 0.74)	22.3 (<0.001)	0.65 (0.54, 0.75)	23.4 (<0.001)
Outer inferior	N=248 (401)	0.56 (0.46, 0.67)	23.0 (<0.001)	0.58 (0.48, 0.68)	23.8 (<0.001)
Spectralis GCC (µm)					
Global	N=248 (401)	1.14 (0.99, 1.29)	34.0 (<0.001)	1.13 (0.98, 1.28)	33.4 (<0.001)
Inner ring	N=248 (401)	1.33 (1.16, 1.51)	34.5 (<0.001)	1.32 (1.15, 1.49)	33.9 (<0.001)
Outer ring	N=248 (401)	0.95 (0.81, 1.08)	29.1 (<0.001)	0.94 (0.81, 1.08)	28.6 (<0.001)
Inner temporal	N=248 (401)	1.41 (1.23, 1.59)	37.5 (<0.001)	1.41 (1.23, 1.59)	37.0 (<0.001)
Inner superior	N=248 (401)	1.12 (0.91, 1.32)	20.9 (<0.001)	1.10 (0.89, 1.31)	20.2 (<0.001)
Inner nasal	N=248 (401)	1.10 (0.90, 1.29)	20.8 (<0.001)	1.09 (0.89, 1.28)	20.2 (<0.001)
Inner inferior	N=248 (401)	1.64 (1.41, 1.87)	32.8 (<0.001)	1.63 (1.39, 1.86)	32.2 (<0.001)
Outer temporal	N=248 (401)	0.78 (0.66, 0.91)	28.0 (<0.001)	0.78 (0.66, 0.90)	27.3 (<0.001)
Outer superior	N=248 (401)	0.95 (0.77, 1.13)	20.8 (<0.001)	0.94 (0.76, 1.12)	20.4 (<0.001)
Outer nasal	N=248 (401)	1.09 (0.91, 1.27)	22.9 (<0.001)	1.08 (0.90, 1.26)	22.4 (<0.001)
Outer inferior	N=248 (401)	0.96 (0.79, 1.13)	22.4 (<0.001)	0.96 (0.79, 1.14)	22.1 (<0.001)
Avanti GCC (µm)					
Whole image	N=204 (317)	1.23 (1.05, 1.42)	31.2 (<0.001)	1.23 (1.04, 1.42)	30.9 (<0.001)
Parafovea	N=204 (317)	1.33 (1.13, 1.53)	31.9 (<0.001)	1.32 (1.12, 1.52)	31.6 (<0.001)
Temporal	N=204 (317)	1.42 (1.21, 1.63)	35.7 (<0.001)	1.41 (1.20, 1.62)	35.4 (<0.001)
Superior	N=203 (316)	1.13 (0.88, 1.37)	18.9 (<0.001)	1.12 (0.87, 1.37)	18.6 (<0.001)
Nasal	N=204 (317)	1.11 (0.90, 1.32)	20.2 (<0.001)	1.10 (0.89, 1.32)	20.0 (<0.001)
Inferior	N=204 (316)	1.67 (1.40, 1.93)	32.3 (<0.001)	1.65 (1.39, 1.92)	31.9 (<0.001)
Avanti Vessel Density (%)					
Whole image	N=204 (317)	0.46 (0.38, 0.53)	31.1 (<0.001)	0.44 (0.37, 0.52)	31.8 (<0.001)
Parafovea	N=204 (317)	0.48 (0.40, 0.56)	31.0 (<0.001)	0.47 (0.39, 0.54)	31.9 (<0.001)
Temporal	N=204 (317)	0.50 (0.42, 0.59)	31.7 (<0.001)	0.49 (0.41, 0.58)	31.6 (<0.001)
Superior	N=203 (316)	0.42 (0.33, 0.50)	21.6 (<0.001)	0.40 (0.32, 0.49)	22.1 (<0.001)
Nasal	N=204 (317)	0.39 (0.31, 0.48)	19.9 (<0.001)	0.38 (0.30, 0.47)	20.3 (<0.001)
Inferior	N=204 (316)	0.62 (0.53, 0.72)	32.8 (<0.001)	0.61 (0.51, 0.70)	33.2 (<0.001)
Spectralis Choroid (µm)					
Global	N=247 (400)	0.35 (-0.11, 0.80)	0.3 (0.137)	0.25 (-0.19, 0.69)	0.2 (0.262)
Inner Ring	N=247 (400)	0.51 (-0.04, 1.06)	0.5 (0.068)	0.39 (-0.13, 0.92)	0.4 (0.144)
Outer Ring	N=247 (400)	0.31 (-0.14, 0.75)	0.2 (0.177)	0.21 (-0.22, 0.63)	0.2 (0.335)
Inner Temporal	N=247 (400)	0.43 (-0.17, 1.04)	0.4 (0.159)	0.27 (-0.30, 0.85)	0.2 (0.355)
Inner Superior	N=247 (400)	0.67 (0.01, 1.33)	0.7 (0.046)	0.49 (-0.14, 1.12)	0.5 (0.127)
Inner Nasal	N=247 (400)	0.77 (0.10, 1.44)	0.8 (0.025)	0.59 (-0.05, 1.22)	0.6 (0.071)
Inner Inferior	N=247 (400)	0.48 (-0.14, 1.10)	0.4 (0.130)	0.33 (-0.26, 0.93)	0.2 (0.274)
Outer Temporal	N=247 (400)	0.40 (-0.09, 0.88)	0.5 (0.108)	0.25 (-0.20, 0.71)	0.3 (0.281)
Outer Superior	N=247 (400)	0.27 (-0.33, 0.88)	0.1 (0.376)	0.12 (-0.46, 0.69)	0.0 (0.687)
Outer Nasal	N=247 (400)	0.34 (-0.20, 0.87)	0.2 (0.217)	0.18 (-0.32, 0.69)	0.1 (0.477)
Outer Inferior	N=247 (400)	0.46 (-0.11, 1.02)	0.4 (0.118)	0.32 (-0.23, 0.86)	0.2 (0.253)

Table 3. Ocular characteristics associations with Visual Field mean deviation

*Linear mixed models slope estimates (with 95% confidence intervals) from univariable and multivariable models adjusted for age and axial length.

^R^2 reported as a percentage

Abbreviations: GCC; Ganglion cell complex, GCIPL; Ganglion cell inner plexiform layer, RNFL; Retinal nerve fiber layer

Secondary Analysis of Differences by Axial Myopia Group

As a secondary analysis, we compared macular thickness- and vascular measurement differences across the three axial myopia groups and adjusted for age and VFMD. In general, mRNFL was thickest in high myopic eyes in all sectors, while mCT was significantly thinner in all sectors in high myopic eyes. The pattern of other macular thickness and vessel density measurements were less consistent across the three axial myopia groups (Supplemental Table 1 and Figures 2A-2F.)

Specifically, global and sectoral GCC (both Spectralis and Avanti) and GCIPL thickness values were similar across myopic groups, except for the inner and outer nasal rings, and inferior outer ring GCIPL (all p≤0.033) (see Figures 2A, 2C and 2D). Compared to no and mild myopia groups, thicker mRNFL was generally found in high myopes globally and in specific sectors (age and VF adjusted MD global: p=0.031, global inner: p=0.051, global outer p=0.042, inner superior ring p=0.001 and outer superior ring (p=0.017) (Figure 2B). Parafoveal vessel density tended to be slightly higher in non-myopes compared to mild and high myopes, but only reached statistical significance in the nasal sector (mean [95% CI]); nasal vessel density in high myopes (42.7% [40.7%, 44.6%]) and non-myopes (44.5% [43.3%, 45.7%]) (p=0.011) (Figure 2E). Global and sectoral mean MCT was significantly thinner in high myopes compared to mild and non-myopes (all p<0.001, See Figure 2F).

Discussion

The results of this work have implications for diagnosing glaucoma in the challenging patients with high myopia. Specifically, our results suggest that macula measurements can be useful measurements to diagnose and monitor glaucoma in myopic eyes as the GCIPL and GCC thinned with increasing severity of glaucoma but are not associated with axial length. Except for choroidal thickness, all other macula thickness measures obtained in this study were associated with the severity of glaucoma. Because ganglion cell-related macular

thickness measurements are strongly associated with VFMD but do not vary with axial length, GCIPL and GCC show promise for detecting glaucoma in myopic eyes.

Because the macula is devoid of morphometric variations such as tilt and peripapillary atrophy, it's diagnostic role in detecting glaucoma in highly myopic eyes is gaining more attention recently. Specifically, there is evidence that myopia can lead to a high rate of false-positives in the measurement of the peripapillary RNFL (pRNFL).[23] Several studies have examined the diagnostic ability of GCIPL, pRNFL and GCC and reported that GCIPL thickness has been reported as superior [8 9 24-27] or comparable to pRNFL thickness[28] for diagnosing glaucoma in myopic eyes. Shoji et al. found that GCC parameters had high diagnostic accuracy to detect glaucoma in highly myopic eyes and that the diagnostic ability was higher than that of the pRNFL.[8] In another study, these authors reported that GCC parameters were not significantly related to refractive errors and had good accuracy to detect glaucoma in non-myopes and in high myopes.[9] Similarly, Kim et al. determined that in highly myopic eyes, the accuracy of glaucoma detection based on the macular GCC thickness was comparable to that based on the pRNFL thickness.[29] These findings and those of other studies[8 9 27] are consistent with our results that GCIPL and GCC thickness measured using both Spectralis and Avanti showed no association between the GCIPL thickness and axial length suggesting GCIPL thickness is less sensitive to changes due to axial elongation. Moreover, in our study GCIPL and GCC measurements showed the strongest association with VFMD, suggesting that both are useful for measuring ganglion cell loss associated with glaucoma in both non-highly myopic and highly myopic eyes. These results are generalizable across instruments as both Spectralis GCC and Avanti GCC showed similar results.

High myopia is characterized by marked structural changes in the retina and choroid and the corresponding vasculature.[30 31] With the introduction of the non-invasive technique, OCTA images can provide a microvascular map from different retinal layers. To the best of our

knowledge this is the first study comparing both macular tissue thickness and vascular measurements in axial non-myopic, mild and high myopic glaucomatous eyes.

In the current study, the macular vessel density showed a weak association with axial length and a moderate association with VFMD. Previous studies reported conflicting results. This inconsistency can be explained in part by differences in study populations and image acquisition and analysis protocols. For instance, we employed a 3 x 3 mm imaging area whereas Yang et al. employed a larger 6 x 6 mm area.[31] A large scan size can be more sensitive to image artefacts but also may identify microvasculature dropout in outer regions.[31] We found only a weak association between superficial macula vessel density and axial length but a moderate association between vessel density and VFMD. Our results suggest that although myopic changes might affect vessel density in the macula, effects due to glaucoma are much stronger as indicated by the stronger association to the VFMD and therefore may also be useful for monitoring glaucoma in myopic eyes.[32]

In terms of choroidal thickness, as axial length increased, the choroid thinned in all sectors. Previously reported results have demonstrated choroidal thinning in highly myopic eyes.[33-35] Ho et al.[33] reported that subfoveal choroidal thickness decreased by 6.20 µm for each diopter of myopia and was thinnest in the nasal sectors in all groups, which is similar to the distributions of non-axial myopes, mild axial myopes and high axial myopes in our study. The choroid is a highly vascular layer, supplied by the posterior ciliary arteries and provides the retinal photoreceptors and the retinal pigment epithelium with oxygen and nourishment.[36] Our results did not show an association between choroidal thickness and VFMD which suggests that choroidal thickness likely is not a useful metric for differentiating glaucomatous from healthy eyes or for monitoring glaucomatous progression.

The current study has several limitations. First, individuals with high myopia were younger. As retinal tissue is known to thin in older eyes[37] we adjusted for age and VFMD in all analyses. In addition, we compared the 3 axial myopic groups after age-matching and found

similar results (data not shown) with respect to the pattern of the retinal and vascular measurements in the three groups. Second, it has been suggested that axial length might affect retinal vessel density measurements and lead to incorrect scaling in OCTA imaging, which should be taken into account when interpreting our results.[38] Moreover, as vessel density measurements vary across instruments,[39] these sVD results are not necessarily generalizable to macula vessel density measurements from other OCTA instruments or to macula deep layer vessel density measurements. In addition, axial elongation often leads to retinal layer segmentation errors and measurement failures. However, we reviewed the OCT images meticulously for segmentation errors and excluded data with uncorrectable segmentation failures. Finally, the sample size of the high myopic group was relatively small compared to the other two groups and the mean axial length was only 26.5 mm. We can therefore not generalize our results to eyes with longer axial length.

In conclusion, GCIPL and GCC thickness can be useful measurements to diagnose and monitor glaucoma in myopic eyes as they thinned with increasing severity of glaucoma but did not vary with axial length. Macular sVD may also be useful for detecting glaucoma in myopic eyes, however we found a weak association between vessel density and axial length which needs to be explored further.

Funding

Grant support:
JR: German Research Foundation research fellowship grant recipient (RE 4155/1-1) and German Ophthalmological Society Grant
MC: K99EY030942
SM: Tobacco-Related Disease Research Program T31IP1511
RNW: National Eye Institute R01EY029058, an Unrestricted grant from Research to Prevent Blindness (New York, NY)
LMZ: National Eye Institute R01EY011008, R01EY019869, R01EY027510, P30EY022589

Competing Interests:
None: JR, CB, JD, AB, JAP, MC, LH, JBJ, RCP, SM, HH, MAF

RNW: Consulting: Bausch & Lomb, Eyenovia, Aerie Pharmaceuticals, Allergan; Research Funding or Equipment: Bausch & Lomb, Heidelberg Engineering, Carl Zeiss Meditec, Konan Medical, Genentech, Optos, Optovue, Centervue; Patent: Toromedes, Carl Zeiss Meditec-Zeiss

LMZ: Research Funding and Equipment: Heidelberg Engineering; Research Equipment: Optovue Inc, Carl Zeiss Meditec Inc, Topcon Medical Systems Inc; Patent: Carl Zeiss Meditec.

References

1. Marcus MW, de Vries MM, Junoy Montolio FG, et al. Myopia as a risk factor for open-angle glaucoma: a systematic review and meta-analysis. *Ophthalmology* 2011;118(10):1989-94 e2. doi: 10.1016/j.ophtha.2011.03.012 [published Online First: 2011/06/21]
2. Leung CK, Cheung CY, Weinreb RN, et al. Retinal nerve fiber layer imaging with spectral-domain optical coherence tomography: a variability and diagnostic performance study. *Ophthalmology* 2009;116(7):1257-63, 63 e1-2. doi: 10.1016/j.ophtha.2009.04.013 [published Online First: 2009/05/26]
3. Jonas JB, Gusek GC, Naumann GO. Optic disk morphometry in high myopia. *Graefe's archive for clinical and experimental ophthalmology = Albrecht von Graefes Archiv fur klinische und experimentelle Ophthalmologie* 1988;226(6):587-90. doi: 10.1007/BF02169209 [published Online First: 1988/01/01]
4. Leung CK, Mohamed S, Leung KS, et al. Retinal nerve fiber layer measurements in myopia: An optical coherence tomography study. *Investigative ophthalmology & visual science* 2006;47(12):5171-6. doi: 10.1167/iovs.06-0545 [published Online First: 2006/11/24]
5. Leung CK, Yu M, Weinreb RN, et al. Retinal nerve fiber layer imaging with spectral-domain optical coherence tomography: interpreting the RNFL maps in healthy myopic eyes. *Investigative ophthalmology & visual science* 2012;53(11):7194-200. doi: 10.1167/iovs.12-9726 [published Online First: 2012/09/22]
6. Curcio CA, Allen KA. Topography of ganglion cells in human retina. *The Journal of comparative neurology* 1990;300(1):5-25. doi: 10.1002/cne.903000103 [published Online First: 1990/10/01]
7. Hood DC, Raza AS, de Moraes CG, et al. Glaucomatous damage of the macula. *Progress in retinal and eye research* 2013;32:1-21. doi: 10.1016/j.preteyeres.2012.08.003 [published Online First: 2012/09/22]
8. Shoji T, Sato H, Ishida M, et al. Assessment of glaucomatous changes in subjects with high myopia using spectral domain optical coherence tomography. *Investigative ophthalmology & visual science* 2011;52(2):1098-102. doi: 10.1167/iovs.10-5922 [published Online First: 2010/11/06]
9. Shoji T, Nagaoka Y, Sato H, et al. Impact of high myopia on the performance of SD-OCT parameters to detect glaucoma. *Graefe's archive for clinical and experimental ophthalmology = Albrecht von Graefes Archiv fur klinische und experimentelle Ophthalmologie* 2012;250(12):1843-9. doi: 10.1007/s00417-012-1994-8 [published Online First: 2012/05/05]
10. Akashi A, Kanamori A, Nakamura M, et al. The ability of macular parameters and circumpapillary retinal nerve fiber layer by three SD-OCT instruments to diagnose highly myopic glaucoma. *Investigative ophthalmology & visual science* 2013;54(9):6025-32. doi: 10.1167/iovs.13-12630 [published Online First: 2013/08/03]
11. Nakanishi H, Akagi T, Hangai M, et al. Effect of Axial Length on Macular Ganglion Cell Complex Thickness and on Early Glaucoma Diagnosis by Spectral-Domain Optical Coherence Tomography. *Journal of glaucoma* 2016;25(5):e481-90. doi: 10.1097/IJG.0000000000000330 [published Online First: 2015/11/10]
12. Hung KC, Wu PC, Poon YC, et al. Macular Diagnostic Ability in OCT for Assessing Glaucoma in High Myopia. *Optometry and vision science : official publication of the American Academy of Optometry* 2016;93(2):126-35. doi: 10.1097/OPX.0000000000000776 [published Online First: 2015/12/26]
13. Wu J, Sebastian RT, Chu CJ, et al. Reduced Macular Vessel Density and Capillary Perfusion in Glaucoma Detected Using OCT Angiography. *Current eye research* 2019;44(5):533-40. doi: 10.1080/02713683.2018.1563195 [published Online First: 2018/12/24]
14. Moghimi S, Zangwill LM, Penteado RC, et al. Macular and Optic Nerve Head Vessel Density and Progressive Retinal Nerve Fiber Layer Loss in Glaucoma. *Ophthalmology* 2018;125(11):1720-28. doi: 10.1016/j.ophtha.2018.05.006 [published Online First: 2018/06/17]

15. Gupta P, Cheung CY, Saw SM, et al. Peripapillary choroidal thickness in young Asians with high myopia. *Investigative ophthalmology & visual science* 2015;56(3):1475-81. doi: 10.1167/iovs.14-15742 [published Online First: 2015/02/07]
16. Yang H, Luo H, Gardiner SK, et al. Factors Influencing Optical Coherence Tomography Peripapillary Choroidal Thickness: A Multicenter Study. *Investigative ophthalmology & visual science* 2019;60(2):795-806. doi: 10.1167/iovs.18-25407 [published Online First: 2019/02/28]
17. Flores-Moreno I, Lugo F, Duker JS, et al. The relationship between axial length and choroidal thickness in eyes with high myopia. *American journal of ophthalmology* 2013;155(2):314-19 e1. doi: 10.1016/j.ajo.2012.07.015 [published Online First: 2012/10/06]
18. Ikuno Y, Tano Y. Retinal and choroidal biometry in highly myopic eyes with spectral-domain optical coherence tomography. *Investigative ophthalmology & visual science* 2009;50(8):3876-80. doi: 10.1167/iovs.08-3325 [published Online First: 2009/03/13]
19. Sample PA, Girkin CA, Zangwill LM, et al. The African Descent and Glaucoma Evaluation Study (ADAGES): design and baseline data. *Arch Ophthalmol* 2009;127(9):1136-45. doi: 10.1001/archophthalmol.2009.187
20. Ghahari E, Bowd C, Zangwill LM, et al. Macular Vessel Density in Glaucomatous Eyes With Focal Lamina Cribrosa Defects. *J Glaucoma* 2018;27(4):342-49. doi: 10.1097/IJG.0000000000000922 [published Online First: 2018/02/21]
21. Rezapour J, Bowd C, Dohleman J, et al. The influence of axial myopia on optic disc characteristics of glaucoma eyes. *Sci Rep* 2021;11(1):8854. doi: 10.1038/s41598-021-88406-1 [published Online First: 2021/04/25]
22. Hongmei Song, Wenguan Wang, Sanyuan Zhao, Jianbing Shen, Kin-Man Lam; Pyramid Dilated Deeper ConvLSTM for Video Salient Object DetectionProceedings of the European Conference on Computer Vision (ECCV), 2018, pp. 715-731.
23. Biswas S, Lin C, Leung CK. Evaluation of a Myopic Normative Database for Analysis of Retinal Nerve Fiber Layer Thickness. *JAMA Ophthalmol* 2016;134(9):1032-9. doi: 10.1001/jamaophthalmol.2016.2343 [published Online First: 2016/07/22]
24. Seol BR, Jeoung JW, Park KH. Glaucoma Detection Ability of Macular Ganglion Cell-Inner Plexiform Layer Thickness in Myopic Preperimetric Glaucoma. *Investigative ophthalmology & visual science* 2015;56(13):8306-13. doi: 10.1167/iovs.15-18141 [published Online First: 2016/01/01]
25. Kim YK, Yoo BW, Jeoung JW, et al. Glaucoma-Diagnostic Ability of Ganglion Cell-Inner Plexiform Layer Thickness Difference Across Temporal Raphe in Highly Myopic Eyes. *Investigative ophthalmology & visual science* 2016;57(14):5856-63. doi: 10.1167/iovs.16-20116 [published Online First: 2016/11/02]
26. Baek SU, Kim KE, Kim YK, et al. Development of Topographic Scoring System for Identifying Glaucoma in Myopic Eyes: A Spectral-Domain OCT Study. *Ophthalmology* 2018;125(11):1710-19. doi: 10.1016/j.ophtha.2018.05.002 [published Online First: 2018/06/12]
27. Yang Z, Tatham AJ, Weinreb RN, et al. Diagnostic ability of macular ganglion cell inner plexiform layer measurements in glaucoma using swept source and spectral domain optical coherence tomography. *PLoS One* 2015;10(5):e0125957. doi: 10.1371/journal.pone.0125957
28. Choi YJ, Jeoung JW, Park KH, et al. Glaucoma detection ability of ganglion cell-inner plexiform layer thickness by spectral-domain optical coherence tomography in high myopia. *Investigative ophthalmology & visual science* 2013;54(3):2296-304. doi: 10.1167/iovs.12-10530 [published Online First: 2013/03/07]
29. Kim NR, Lee ES, Seong GJ, et al. Comparing the ganglion cell complex and retinal nerve fibre layer measurements by Fourier domain OCT to detect glaucoma in high myopia. *The British journal of ophthalmology* 2011;95(8):1115-21. doi: 10.1136/bjo.2010.182493 [published Online First: 2010/09/02]
30. Ye J, Wang M, Shen M, et al. Deep Retinal Capillary Plexus Decreasing Correlated With the Outer Retinal Layer Alteration and Visual Acuity Impairment in Pathological Myopia. *Investigative*

ophthalmology & visual science 2020;61(4):45. doi: 10.1167/iovs.61.4.45 [published Online First: 2020/04/29]
31. Yang D, Cao D, Zhang L, et al. Macular and peripapillary vessel density in myopic eyes of young Chinese adults. *Clinical & experimental optometry* 2020;103(6):830-37. doi: 10.1111/cxo.13047 [published Online First: 2020/02/14]
32. Lee K, Maeng KJ, Kim JY, et al. Diagnostic ability of vessel density measured by spectral-domain optical coherence tomography angiography for glaucoma in patients with high myopia. *Scientific reports* 2020;10(1):3027. doi: 10.1038/s41598-020-60051-0 [published Online First: 2020/02/23]
33. Ho M, Liu DT, Chan VC, et al. Choroidal thickness measurement in myopic eyes by enhanced depth optical coherence tomography. *Ophthalmology* 2013;120(9):1909-14. doi: 10.1016/j.ophtha.2013.02.005 [published Online First: 2013/05/21]
34. Harb E, Hyman L, Gwiazda J, et al. Choroidal Thickness Profiles in Myopic Eyes of Young Adults in the Correction of Myopia Evaluation Trial Cohort. *Am J Ophthalmol* 2015;160(1):62-71 e2. doi: 10.1016/j.ajo.2015.04.018
35. Wei WB, Xu L, Jonas JB, et al. Subfoveal choroidal thickness: the Beijing Eye Study. *Ophthalmology* 2013;120(1):175-80. doi: 10.1016/j.ophtha.2012.07.048 [published Online First: 2012/09/27]
36. Linsenmeier RA, Padnick-Silver L. Metabolic dependence of photoreceptors on the choroid in the normal and detached retina. *Investigative ophthalmology & visual science* 2000;41(10):3117-23. [published Online First: 2000/09/01]
37. Hammel N, Belghith A, Bowd C, et al. Rate and Pattern of Rim Area Loss in Healthy and Progressing Glaucoma Eyes. *Ophthalmology* 2016;123(4):760-70. doi: 10.1016/j.ophtha.2015.11.018 [published Online First: 2016/01/10]
38. Sampson DM, Gong P, An D, et al. Axial Length Variation Impacts on Superficial Retinal Vessel Density and Foveal Avascular Zone Area Measurements Using Optical Coherence Tomography Angiography. *Investigative ophthalmology & visual science* 2017;58(7):3065-72. doi: 10.1167/iovs.17-21551 [published Online First: 2017/06/18]
39. Li XX, Wu W, Zhou H, et al. A quantitative comparison of five optical coherence tomography angiography systems in clinical performance. *International journal of ophthalmology* 2018;11(11):1784-95. doi: 10.18240/ijo.2018.11.09 [published Online First: 2018/11/20]

Figure Legends

Figure 1: Optic disc photograph (left), optical coherence tomography optic nerve head en face image (middle) and optical coherence tomography macula posterior pole image (right) of an eye with (A) no axial myopia (axial length = 23.8 mm), (B) mild axial myopia (axial length = 24.7 mm and (C) high axial myopia (axial length = 29 mm).

Figure 2: Sectoral and global thickness distribution of the Spectralis GCIPL thickness (1A), Spectralis macular RNFL thickness (1B), Spectralis GCC thickness (1C), Avanti GCC thickness (1D), Avanti macular vessel density (1E) and Spectralis macular choroidal thickness (1F) in non-myopic, mild myopic and highly myopic glaucoma eyes.
Abbreviations: GCC; ganglion cell complex, GCIPL; ganglion cell inner plexiform layer, RNFL; retinal nerve fiber layer

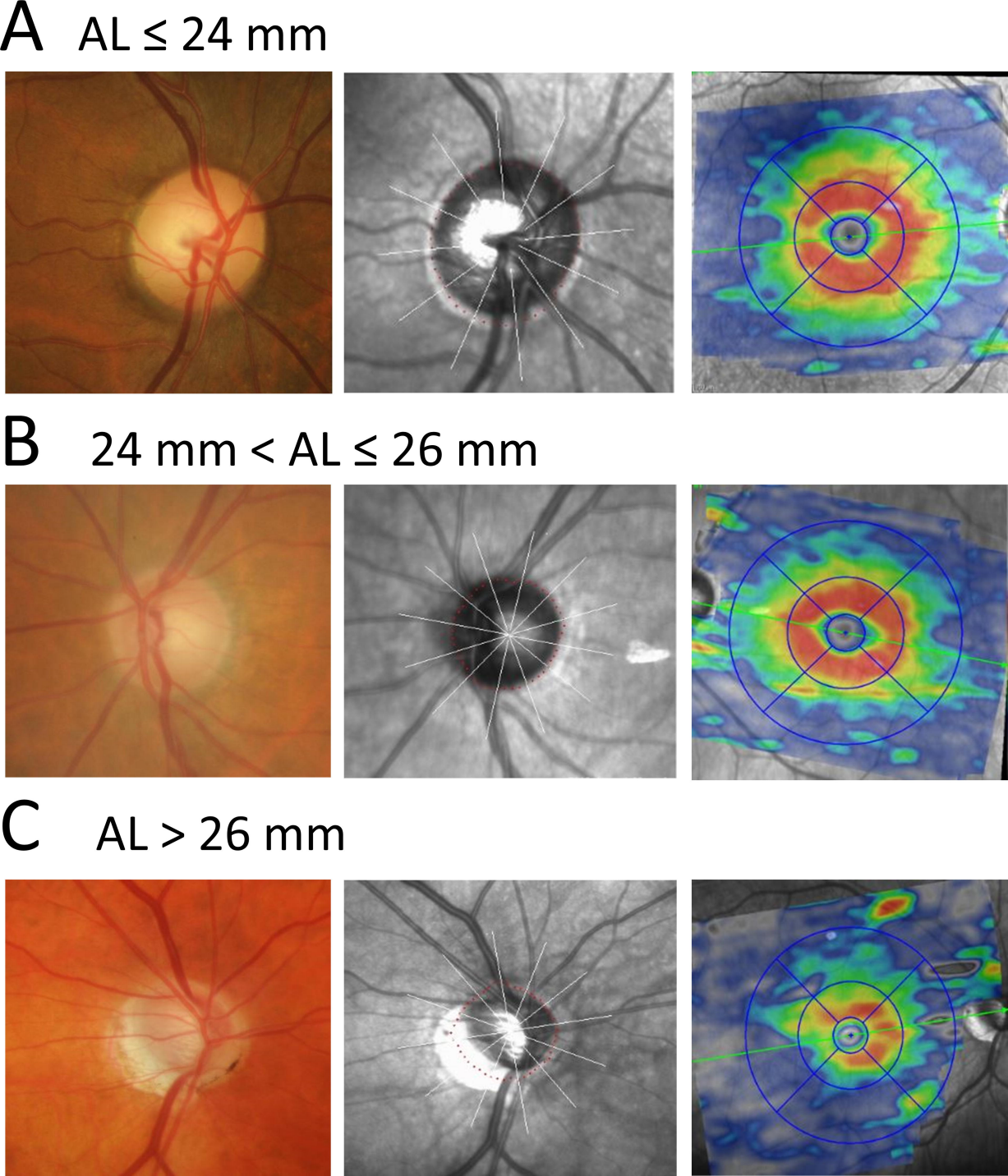
A
AL ≤ 24 mm
B
24 mm < AL ≤ 26 mm
C
AL > 26 mm

A)

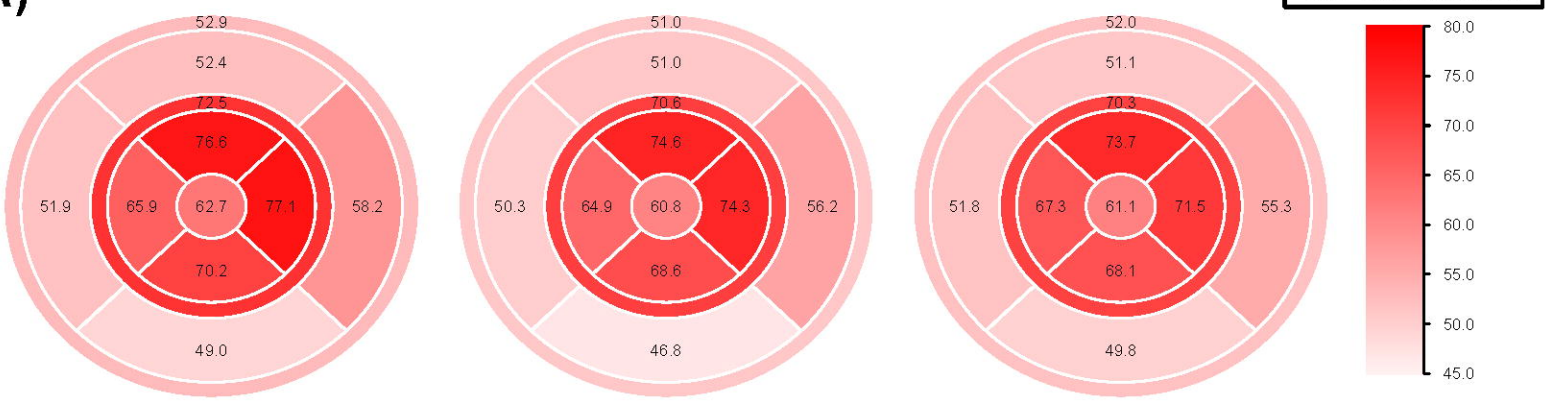
No Myopia
52.9
52.4
72.5
76.6
51.9
65.9
62.7
77.1
58.2
70.2
49.0
Mild Myopia
51.0
51.0
70.6
74.6
50.3
64.9
60.8
74.3
56.2
68.6
46.8
High Myopia
52.0
51.1
70.3
73.7
51.8
67.3
61.1
71.5
55.3
68.1
49.8
Spectralis
GCIPL Thickness (µm)
80.0
75.0
70.0
65.0
60.0
55.0
50.0
45.0

B)

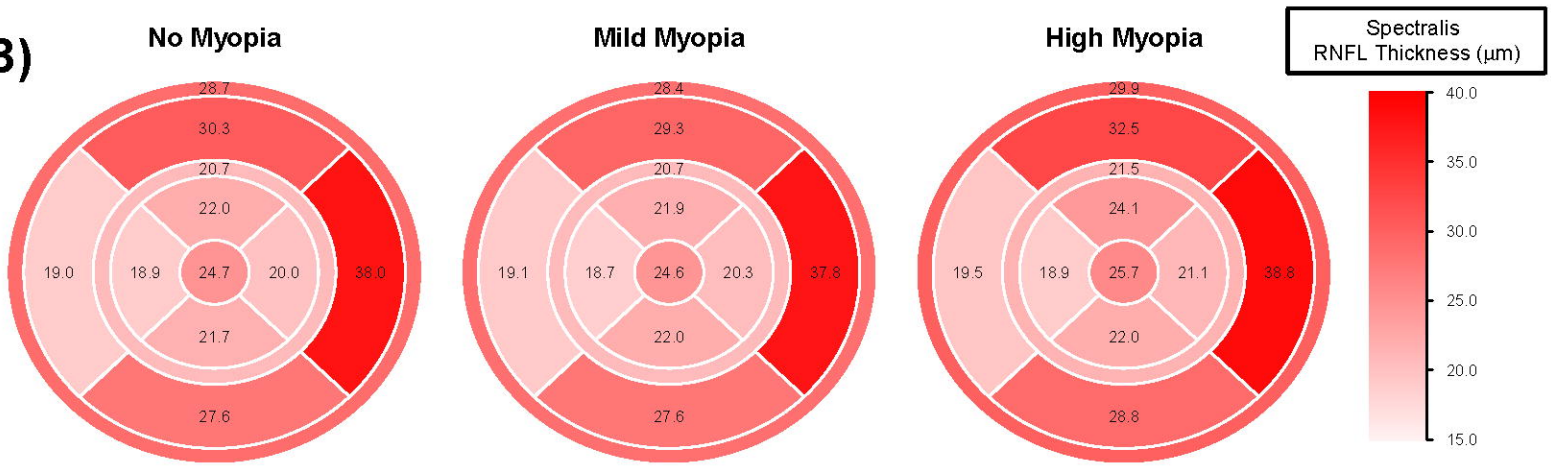
No Myopia
28.7
30.3
20.7
22.0
19.0
18.9
24.7
20.0
38.0
21.7
27.6
Mild Myopia
28.4
29.3
20.7
21.9
19.1
18.7
24.6
20.3
37.8
22.0
27.6
High Myopia
29.9
32.5
21.5
24.1
19.5
18.9
25.7
21.1
38.8
22.0
28.8
Spectralis
RNFL Thickness (µm)
40.0
35.0
30.0
25.0
20.0
15.0

C)

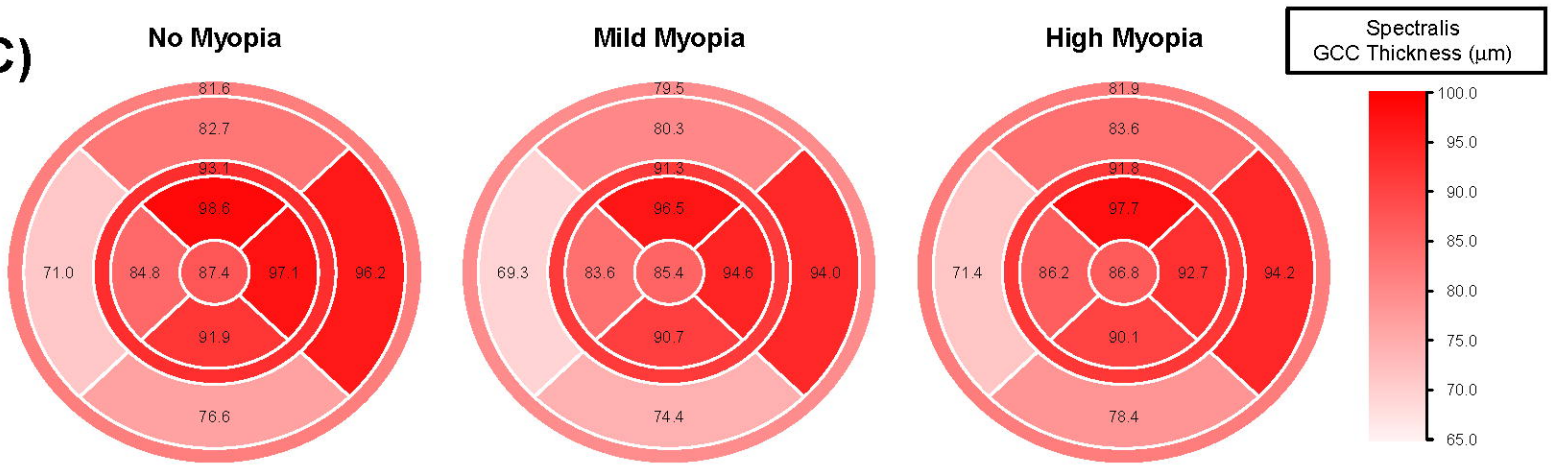
No Myopia
81.6
82.7
93.1
98.6
71.0
84.8
87.4
97.1
96.2
91.9
76.6
Mild Myopia
79.5
80.3
91.3
96.5
69.3
83.6
85.4
94.6
94.0
90.7
74.4
High Myopia
81.9
83.6
91.8
97.7
71.4
86.2
86.8
92.7
94.2
90.1
78.4
Spectralis
GCC Thickness (µm)
100.0
95.0
90.0
85.0
80.0
75.0
70.0
65.0

D)

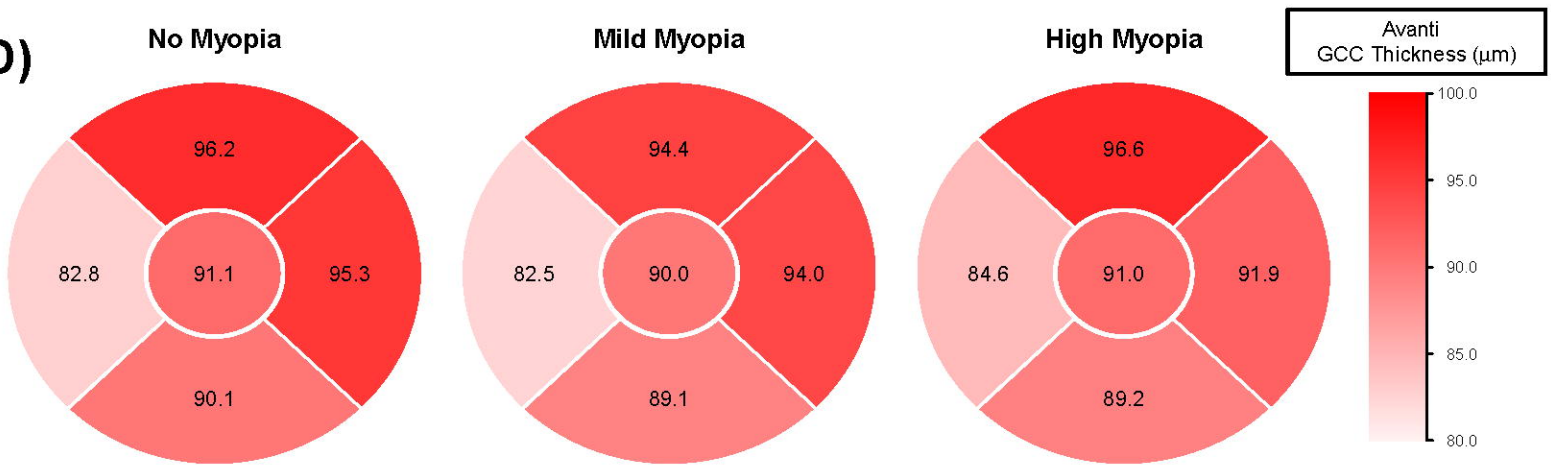
No Myopia
96.2
82.8
91.1
95.3
90.1
Mild Myopia
94.4
82.5
90.0
94.0
89.1
High Myopia
96.6
84.6
91.0
91.9
89.2
Avanti
GCC Thickness (µm)
100.0
95.0
90.0
85.0
80.0

E)

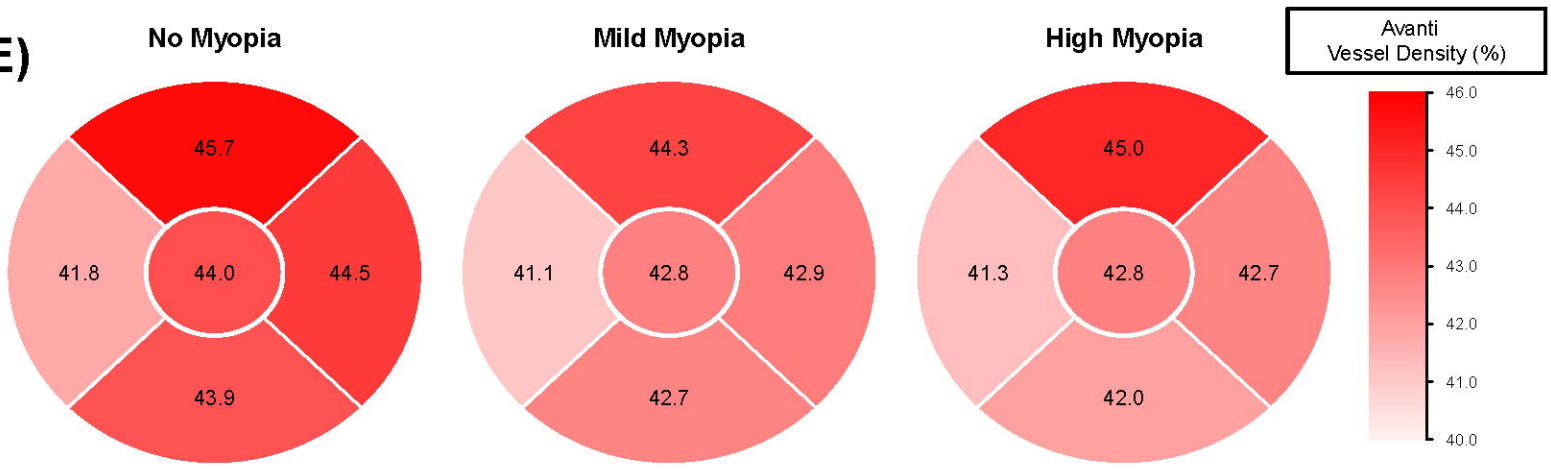
No Myopia
45.7
41.8
44.0
44.5
43.9
Mild Myopia
44.3
41.1
42.8
42.9
42.7
High Myopia
45.0
41.3
42.8
42.7
42.0
Avanti
Vessel Density (%)
46.0
45.0
44.0
43.0
42.0
41.0
40.0

F)

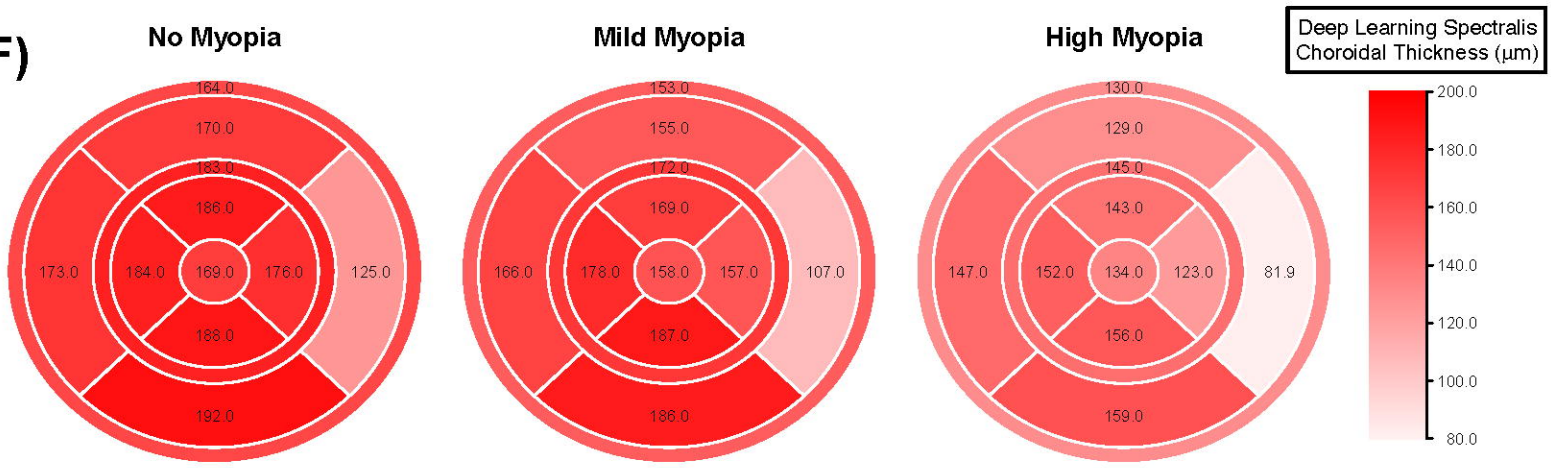
No Myopia
164.0
170.0
183.0
186.0
173.0
184.0
169.0
176.0
125.0
188.0
192.0
Mild Myopia
153.0
155.0
172.0
169.0
166.0
178.0
158.0
157.0
107.0
187.0
186.0
High Myopia
130.0
129.0
145.0
143.0
147.0
152.0
134.0
123.0
81.9
156.0
159.0
Deep Learning Spectralis
Choroidal Thickness (µm)
200.0
180.0
160.0
140.0
120.0
100.0
80.0